Vegetable oil-based hybrid microparticles as a green and biocompatible system for subcutaneous drug delivery

Koceïla Doufène, Ilaria Basile, Aurélien Lebrun, Nelly Pirot, Aurélie Escande, Joel Chopineau, Jean-Marie Devoisselle, Nadir Bettache, Anne Aubert-Pouëssel

Vegetable Oil-based Hybrid Microparticles as a Green and Biocompatible System for Subcutaneous Drug Delivery

Koceïla Doufène [a], *Ilaria Basile* [b], *Aurélien Lebrun* [c], *Nelly Pirot* [d,e], *Aurélie Escande* [f], *Joël Chopineau* [a], *Jean-Marie Devoisselle* [a], *Nadir Bettache* [g] *and Anne Aubert-Pouëssel* [a]*

[a] Institut Charles Gerhardt Montpellier (ICGM), Univ. Montpellier, CNRS, ENSCM, Montpellier, France.

[b] NanoMedSyn, Montpellier, France.

[c] Laboratoire des Mesures Physiques (LMP), Univ. Montpellier, CNRS, Montpellier, France.

[d] Institut de Recherche en Cancérologie de Montpellier (IRCM), Univ. Montpellier, ICM, INSERM, Montpellier, France.

[e] BioCampus Montpellier (BCM), Univ. Montpellier, CNRS, INSERM, Montpellier, France.

[f] Hydrosciences Montpellier (HSM), Univ. Montpellier, CNRS, IRD, Montpellier, France.

[g] Institut des Biomolécules Max Mousseron (IBMM), Univ. Montpellier, CNRS, ENSCM, Montpellier, France.

* Email Address: anne.aubert@umontpellier.fr

Abstract

The aim of this study was to evidence the ability of vegetable oil-based hybrid microparticles (HMP) to be an efficient and safe drug delivery system after subcutaneous administration. The HMP resulted from combination of a thermostabilized emulsification process and a sol-gel chemistry. First of all, castor oil was successfully silylated by means of (3-Isocyanatopropyl)trimethoxysilane in solvent-free and catalyst-free conditions. Estradiol, as a model drug, was dissolved in silylated castor oil (ICOm) prior to emulsification, and then an optimal sol-gel crosslinking was achieved inside the ICOm microdroplets. The resulting estradiol-loaded microparticles were around 80 µm in size and allowed to entrap 4 wt.% estradiol. Their release kinetics in a PBS/octanol biphasic system exhibited a one-week release profile, and the released estradiol was fully active on HeLa ERE-luciferase ERα cells. The hybrid microparticles were cytocompatible during preliminary tests on NIH 3T3 fibroblasts (ISO 10993-5 standard) and they were fully biocompatible after subcutaneous injection on mice (ISO 10993-6 standard) underlining their high potential as a safe and long-acting subcutaneous drug delivery system.

Keywords

Vegetable oil; green process; sol-gel; estradiol; subcutaneous drug delivery; biocompatible

Abbreviations

API: active pharmaceutical ingredient = drug

CO: castor oil

CD: condensation degree

CY: condensation yield

EC_{50}: half-maximal effective concentration

ERα: estrogen receptor alpha

HELN: HeLa Estrogen Response Element (ERE)-luciferase

HES: hematoxylin-eosin-saffron

HMBC: heteronuclear multiple bond correlation

HMP: hybrid microparticles

HMPe / HMPm: hybrid microparticles made of ICOe or ICOm, respectively

HSQC: heteronuclear single quantum coherence

ICOe / ICOm: castor oil silylated by means of IPTES or by IPTMS, respectively

IPTES: (3-Isocyanatopropyl)triethoxysilane

IPTMS: (3-Isocyanatopropyl)trimethoxysilane

PBS: phosphate buffer saline

PLGA: poly(lactic-co-glycolic acid)

RS: red sirius

SC: subcutaneous

T^x: condensation state of the hydrolyzed trialkoxysilanes depending on the number of the siloxane (Si-O-Si) generated bonds: (T^0, T^1, T^2, and T^3)

1. Introduction

The therapeutic management of chronic diseases is a tricky challenge for both healthcare professionals and their patients. Although most of the drugs prescribed are orally administered, some formulation constraints (e.g. pH-sensitive active pharmaceutical ingredients (APIs)) and the non-compliance of some patients (e.g. mental disorders) may require alternative routes of administration (Sav et al., 2015). In these cases, the subcutaneous (SC) delivery of APIs offers a valuable alternative. Indeed, it is a relatively low-cost route compared to the intravenous one, it is safe, effective, and it allows patient self-administration (Jones et al., 2017). Nevertheless, the scientific community has agreed on the critical need for the development of new technologies and systems in this area (Collins et al., 2020). Indeed, the SC route is relatively unexplored and there is still plenty of room for improvement through long-acting delivery systems (Chen et al., 2018) and systems dedicated to biotherapeutics (e.g. antibodies, insulin and antibiotics) (Bittner et al., 2018; Hernández-Ruiz et al., 2020; P.V. et al., 2017; Viola et al., 2018).

For a long time, injectable oils have been used to deliver APIs such as antipsychotics and steroid hormones (Gao et al., 1995; Kalicharan et al., 2017; Vintiloiu and Leroux, 2008). Among the used oils, castor oil (CO) and its derivatives (hydrogenated and polyoxylated CO) have been widely introduced in parenteral formulations since their approval by the US-FDA (Strickley, 2004). While the derivatives are used as hydrophilic surfactants in aqueous formulations, native CO is used to formulate oily depots for the sustainable release of poorly water-soluble APIs. Indeed, Riffkin et *al.* pointed out as early as the 1960s the interest of using CO as a parenteral vehicle for steroids (Riffkin et al., 1964). This oil in particular offers a greater API solubilization capacity and an improved safety. Furthermore, we highlighted in a previous paper that silylated CO (ICO) synthesized with the aim of a further sol-gel crosslinking kept its solubilizing capacity of poorly water-soluble APIs. ICO was able to

solubilize up to 160 mg of ibuprofen per milliliter and the hybrid microparticles (HMP) obtained after crosslinking of the ICO exhibited an interesting sustained release of ibuprofen in a subcutaneous simulated medium (Doufène et al., 2019).

In this present study, the chemistry of CO silylation was redesigned in order to improve the "green" conditions of HMP synthesis, i.e. in solvent-free and catalyst-free conditions. Estradiol (LogP = 4.01) was used as a model for poorly water-soluble APIs from the broad chemical family of steroids that includes corticosteroids and contraceptives. A comprehensive characterization of the new estradiol-loaded HMP is exposed with an emphasis on estradiol release kinetics, the *in vitro* activity of the released estradiol, and the *in vivo* biocompatibility of the HMP evaluated on mice.

2. Materials and methods

2.1. Materials

Pharmaceutical grade castor oil (CO, 934 $g \cdot mol^{-1}$) was purchased from Cooper Pharmaceutique. (3-Isocyanatopropyl)trimethoxysilane (IPTMS, 205 $g \cdot mol^{-1}$), κ-carrageenan, estradiol (272 $g \cdot mol^{-1}$) and solvents (acetonitrile, acetic acid, methanol and octanol) were supplied by Sigma-Aldrich.

HeLa ERE-luciferase (HELN) ERα cell line aimed to *in vitro* activity assays was kindly donated by the team of Prof. P. Balaguer (Institut de Recherche en Cancérologie de Montpellier - Inserm U1194), and NIH 3T3 fibroblast cell line aimed to cytocompatibility assays was obtained from ATCC. Their culture media were purchased from Thermofisher.

2.2. Synthesis and characterization of silylated castor oil

2.2.1. Synthesis of silylated castor oil

IPTMS was grafted as a silylating agent on castor oil following an isocyanate-hydroxyl reaction in solvent-free and catalyst-free conditions as follows: 15 g of castor oil (containing one molar equivalent of hydroxyl groups (-OH)) were silylated with 7.58 g IPTMS (containing 0.8 molar equivalent of isocyanate groups (-N=C=O)) during 72 h at 60 °C, under nitrogen atmosphere. The silylation ratio 0.8 (i.e., ratio between the quantity of –N=C=O groups in the silylating agent, and –OH groups in the oil) was selected from our previous study (Doufène et al., 2019) because of the lowest toxicity of the resulting HMP on NIH 3T3 fibroblasts and their interesting pharmacotechnical qualities (i.e. hardness and flow properties of the HMP powder). The IPTMS was chosen to replace the (3-Isocyanatopropyl)triethoxysilane (IPTES) previously used to functionalize castor oil then to obtain ICOe. Indeed, IPTMS is a better sol-gel reactive agent (Loy et al., 2000) that could enhance the reactivity of the new silylated castor oil referred to as ICOm. In short, it allows the synthesis of hybrid particles without the use of any metallic catalyst.

2.2.2. Characterization of the silylated castor oil

^{1}H, ^{13}C and ^{29}Si NMR analyses (Bruker Avance III 500 and 600 MHz equipped with cryoprobes) were performed on ICOm in order to determine its structure. The methodology was as follows: the NMR spectra were recorded at 298 K on a Bruker Avance III 600 MHz NMR spectrometer, using TCI Cryoprobe Prodigy®. Chemical shift data were given in δ ppm calibrated with residual protic solvent (e.g. $CDCl_3$: 7.26 ppm -^{1}H / 77.16 ppm – ^{13}C). 2D heteronuclear spectra ^{1}H-^{13}C g-edited HSQC (Heteronuclear Single Quantum Coherence) and ^{1}H-^{13}C g-HMBC (Heteronuclear Multiple Bond Correlation) were acquired to assign the compound (8 - 16 scans, 512 real (t1) × 2048 (t2) complex data points). 2D heteronuclear spectra ^{1}H-^{29}Si g-HMBC (16 scans, 512 real (t1) × 2048 (t2) complex data points) was

obtained on a Bruker Avance III 500 MHz NMR spectrometer, using BroadBand Observable helium cryoprobe in order to establish presence of transesterification on silicium positions. Spectra were processed and visualized with Topspin 3.6.2 (Bruker Biospin) on a Linux station. $CDCl_3$ was purchased from Aldrich. For the quantitative determination of x, y, and z substituent ratios (explained in the result section), the various "CH" were identified by 2D NMR g-edited HSQC ^{13}C and g-HMBC ^{13}C and then integrated on 1D ^{1}H NMR. The ICOm was synthesized and analyzed in triplicate for the purpose.

Furthermore, the viscosity of ICOm was measured with a rotative rheometer (RM 200 Rheomat, Lamy Rheology) equipped with a DIN33 measuring system.

2.3. Formulation and characterization of hybrid microparticles

2.3.1 Microparticle synthesis

The ICOm-based hybrid microparticles (referred to as HMPm) were formulated following the thermostabilized emulsion process we developed (Doufène et al., 2019). Estradiol, as a representative API of the steroid class, was dissolved at 4 wt.% in the ICOm, An aqueous phase composed of an acetate buffer (pH = 2.8) and 0.5 wt.% ƙ-carrageenan was prepared, and the presence of the latter allows it to be liquid above 60 °C and gelled under 25 °C. The oily solution was emulsified in the heated aqueous phase (60 °C) by means of a T 18 digital Ultraturrax® (IKA) at 9000 rpm during 2 min. In order to induce the gelation of the aqueous phase, the temperature was dropped in an ice bath for 5 min. The stabilized emulsion was kept at room temperature for 8 days to allow the sol-gel crosslinking inside the oil microdroplets, and the emulsion to turn into a suspension of HMPm. To recover the particles, the gelled aqueous phase was liquefied by heating at 60 °C, and the resulting HMPm were washed by means of milli-Q water then freeze-dried.

158 **2.3.2 Microparticle characterization**

159 The synthesized microparticles were characterized by complementary techniques to study
160 their morphology (i.e. granulometry using a Mastersizer 2000 from Malvern instruments),
161 their structure (i.e. solid-state ^{29}Si NMR using a Varian VNMRS 400 MHz [9.4T] NMR
162 spectrometer equipped with a 7.5 mm Varian T3 HX MAS probe spinning at 5 kHz;
163 thermogravimetric analysis using STA 6000 from PerkinElmer) and their effective loading of
164 estradiol. The theoretical loading of estradiol was 4 wt.%, i.e. the amount of estradiol
165 solubilized in ICOm, whereas the effective loading of estradiol was equal to the mass of
166 estradiol divided by the mass of the HMPm, and it was determined using a liquid
167 chromatography assay after estradiol extraction (LC-2010HT Shimadzu: static phase =
168 C18 Protonsil® column from Bischoff, mobile phase = acetonitrile/Milli-Q water, 40/60, v/v).
169 The reader is directed to the reference (Doufène et al., 2019) for further technical details.
170

171 ## 2.4. *In vitro* release of estradiol

172 Release tests of estradiol from HMPm were carried out in a flow-through cell apparatus
173 and a biphasic system was chosen to mimic the *in vivo* release of estradiol after SC
174 administration, as depicted in Fig. 1. Indeed, the biphasic systems were extensively reported
175 in literature as of great interest in the study of the *in vitro* release of poorly water-soluble API
176 (Denninger et al., 2020; Phillips et al., 2012a, 2012b) and in the correlation with the *in vivo*
177 behavior of the drug delivery system (Al Durdunji et al., 2016). The used system consisted of
178 200 ml PBS buffer at pH = 7.4 and T = 37 °C as a biorelevant phase flowing at 4 $ml \cdot min^{-1}$ in
179 contact with the sample (40 mg of estradiol-loaded HMPm, containing 5.874 µmol of
180 estradiol) that was entrapped in a flow-through cell. As a storage phase that entraps the
181 estradiol released from the HMPm, 40 ml of octanol at room temperature were used. The very
182 high affinity of estradiol for octanol rather than for water caused all the estradiol released in

PBS to be entrapped in the organic phase, and thus it ensured the sink conditions (LogP (estradiol) = 4.01, meaning that the partition coefficient of estradiol in octanol : water mixture is 10233 : 1, respectively). At determined intervals, samples of the organic phase were analyzed by liquid chromatography as described above, and then a percentage curve of released estradiol over time was drawn from triplicate tests.

(Fig. 1)

2.5. *In vitro* activity assays of released estradiol

2.5.1. Cell line

In order to check the activity of the estradiol released from HMPm and thus to ensure the suitability of the process for drug loading, an already established cell model was used: HELN cell line expressing the estrogen receptor alpha (ERα) (Bellet et al., 2012; Delfosse et al., 2012) that exhibits estradiol-induced Erα activity (Fig. S.1). Briefly, HELN ERα cells were obtained by stably expressing the ERα DNA binding domain in HELN cells.

The HELN ERα cells were cultured in Dulbecco's Modified Eagle Medium without phenol red (DMEM/F-12) supplemented with 5 % steroid free fœtal bovine serum, 1 $g \cdot ml^{-1}$ glucose, 100 $units \cdot ml^{-1}$ of penicillin, 100 $\mu g \cdot ml^{-1}$ of streptomycin, 0.5 $\mu g \cdot ml^{-1}$ puromycin and 1 $mg \cdot ml^{-1}$ geneticin in a 5 % CO_2 humidified atmosphere at 37 °C.

2.5.2. Extract preparation

Unloaded and estradiol-loaded HMPm (freshly synthesized, or stored 12 months at 25 °C and referred to as "old HMPm") were suspended in culture medium (10 mg in 50 ml) and the samples were gently shaken during 24 h at 37 °C. After centrifugation, the supernatants (referred to as extracts) were analyzed by HPLC to determine the amount of released estradiol. On the other hand, solutions of pure estradiol in dimethyl sulfoxide (10^{-5} to 10^{-12} M) were prepared and used as references.

2.5.3. Transactivation experiments

The cells were seeded at a density of 25000 cells per well in 96-well white opaque tissue culture plates (Greiner CellStar) in the aforementioned medium and conditions. The extracts were diluted in the culture medium according to defined concentrations of estradiol (10^{-5} to 10^{-12} M) and added to the cells. After 16 h of co-incubation, the diluted extracts were replaced with test medium containing 0.3 mM luciferin. Luciferase activity was measured for 2 s in intact living cells using a MicroBeta Wallac luminometer (PerkinElmer). Tests were performed in quadruplicate in at least three independent experiments. Data were expressed as a percentage of the theoretical maximal activity of pure estradiol and were given as the mean ± SD.

Agonistic activity of the ERα was tested in presence of increasing concentrations of extracted estradiol. For each sample, the potency corresponding to the concentration yielding half-maximal luciferase activity (EC_{50} value) was determined using the dose/response fitting on Origin® software.

2.6. Cytocompatibility assays

Cytocompatibility assays of unloaded HMPm were conducted according to the ISO 10993-5 standard. Various concentrations of HMPm (0, 0.1, 1 and 10 $mg \cdot ml^{-1}$) were infused in DMEM culture medium during 48 h then centrifuged. The NIH 3T3 fibroblasts (cultured in the same medium and seeded at 5000 cells per well in 96-well plate) were exposed to the extracts, and the viability of the cells was checked after 24 and 48 h using a CellTiter 96® AQ cell proliferation assay (Promega). This test was composed of a tetrazolium compound (3-(4,5-dimethylthiazol-2-yl)-5-(3-carboxymethoxyphenyl)-2-(4-sulfophenyl)-2H-tetrazolium, inner salt; MTS) and an electron coupling reagent (phenazine methosulfate; PMS), and it was used as follows: 20 µl of a mixture MTS-PMS was added in each well for 3 h reaction with

233 the cells, then the assay plate was read at 490 nm using a microplate reader (Multiskan Go,
234 Thermo Fisher Scientific). Finally, cell viability rates were normalized to the absorbance
235 values of the negative control cells (100 % viability), the results are given as the mean ± SD
236 of three independent experiments and statistical analysis was performed using the Student's t-
237 test on Minitab® software.
238
239 **2.7. Biocompatibility assays**
240 Biocompatibility assays of unloaded HMPm were conducted according to the ISO 10993-6
241 standard.
242 **2.7.1. Treatment of the animals**
243 18 BALB/cAnNRj albino male mice (Janvier Labs, France) 10 weeks aged weighting
244 26.1 ± 1.4 g were used for the experiment. The mice were cared for in accordance with the
245 ethical guidelines and the standard protocol was approved by the Committee on the Ethics of
246 Animal Experiments of Languedoc-Roussillon C2EA-36 (reference: #23448-
247 2019122017024717). Before injection, the mice had back hairs shaved and were disinfected
248 with chlorhexidine. The mice were divided into 4 experimental groups with two injected
249 preparations (either the vehicle defined hereafter, or the unloaded HMPm suspended in the
250 vehicle), and with two experiment time-points (4 or 28 days).
251 The unloaded HMPm were sterilized through exposure to UVC rays (Bio-Link 254 nm
252 from Vilber Lourmat, France), then suspended at 25 $mg \cdot ml^{-1}$ in an apyrogenic, isotonic
253 aqueous solution containing 1.5 wt.% carboxymethylcellulose and 0.1 wt.%
254 polysorbate 80. A single dose containing 8 mg of HMPm was injected in the SC space
255 behind the neck of the mouse. The same preparation without HMPm, referred to as
256 "vehicle", was used for the control group.
257

2.7.2. Sample collection and data analysis

At the two time-points (day 4 and day 28), mice were euthanized and their dorsal skin was carefully resected in the injection site. The skin samples were fixed in 4 % formaldehyde solution for 24 h at room temperature and embedded in paraffin. 3 µm thick sections were cut and stained with hematoxylin-eosin-saffron (HES) and red sirius (RS). The scoring criteria permitted to evaluate local tissue effects according to the aforementioned ISO standard. The grading system was performed by a veterinary pathologist as follows: 0 = none, 1 = mild, 2 = moderate, 3 = marked, and 4 = severe.

3. Results and discussion

3.1. Characterization of the silylated castor oil

In order to elucidate the structure of the newly synthesized ICOm, a wide range of NMR experiments were performed (see Fig. S.2 to S.6 in supplementary data). Four types of CH-O were identified, and they were assigned to “CH-O” of the glycerol part, “CH-OH” of the non-silylated branch, “CH-O-IPTMS” of the silylated branch, and the transesterified form “CH-O-Si” (see Fig. S.7 and Table S.1 in supplementary data). Then the percentages x, y and z, depicted in Fig. 2 were determined by integration on 1D ^{1}H NMR using the “CH-O” of the glycerol part as reference, even if the measurement of x was slightly imprecise because of overlapped signals on this area. The results were as follows: x = 9.7 % (± 0.6), y = 62 % (± 0.4) and z = 28.3 % (± 0.2).

(Fig. 2)

Overall, a complete silylation was reached and no early crosslinking was detected as underlined by the absence of Si-O-Si bridge signals on Fig. S.6, but an unexpected reaction between some methoxysilane groups of IPTMS and free hydroxyl groups of castor oil was

pointed out by a non-negligible z percentage, in contrast with the results previously obtained during the silylation with IPTES. It can be explained by the high reactivity of the methoxysilanes that are well-known to induce interfering reactions. However, the narrow standard deviations on the triplicate demonstrate the reproducibility of the results and the mastering of the silylation process.

To highlight the physical impact of the transesterification reaction, the viscosities of ICOm and ICOe were compared. The viscosity of ICOm had a value of 3180 mPa·s while that of ICOe was 764 mPa·s, showing a considerable increase of approximately 4-fold. In the absence of early sol-gel crosslinking, the high viscosity value can only be explained by the formation of ICOm oligomers, which are linked by the urethane group and by the Si-O-C bridge.

3.2. Physicochemical characterization of the hybrid microparticles

The resulting HMPm exhibited a spherical morphology and a micrometric size. Their volume median diameter was around 83 µm (span = 1.43) and was slightly higher than that of HMPe (i.e. HMP made of ICOe, around 55 µm) as previously reported (Doufène et al., 2019). This size increase was due to the higher viscosity of ICOm compared to ICOe. The tendency was confirmed by the higher volume moment mean D[4,3] (89 µm), whereas the surface-area moment mean D[3,2] was 38 µm reflecting a high number of small particles.

The organic/inorganic hybrid structure of HMPm was attested by a mineral residue of approximately 6 % after heating up to 800 °C (Fig. S.8). The formation of siloxane bonds between the silylated fatty acid chains by sol-gel reaction is behind this crosslinked structure. The density of this hybrid structure was then investigated by solid-state ^{29}Si NMR. As indicated in Table 1, the condensation yield (CY) and degree (CD) were 85 % and 79 % respectively, and they were in the same range with those of HMPe at the same silylation ratio

(Doufène et al., 2019). However, the condensation behavior was different as evidenced by the analysis of the various T^x, i.e. the condensation state of the hydrolyzed trialkoxysilanes, depending on the number of siloxane (Si-O-Si) generated bonds (T^0, T^1, T^2, and T^3). Indeed, the amount of T^3 was slightly higher for HMPm (44 %) than for HMPe (36 %), meaning that a higher amount of silicon parts fully crosslinked, and it was due to the better sol-gel reactivity of trimethoxysilanes than triethoxysilanes. In fact, the former are more able to form multiple siloxane bonds since the steric hindrance and the electro-donor inductive effect of the methyl residue are lower on the silicium center (Si) than those of the ethyl one. Overall, a better sol-gel crosslinking efficiency was ensured for these new particles despite the absence of a tin catalyst, and a more sustained API release might be expected.

(Table 1)

Furthermore, the effective loading of estradiol within HMPm showed a value of 4.29 ± 0.18 wt.% slightly higher than the theoretical one (4 wt.%) pointing out a concentration effect of estradiol inside HMPm that occurred during the formulation process. This phenomenon was explained by methanol evaporation during the sol-gel hydrolysis reaction (Doufène et al., 2019).

3.3. *In vitro* release kinetics of estradiol

(Fig. 3)

As depicted in Fig. 1, release kinetics of estradiol from HMPm were carried out in a PBS/octanol biphasic system. The data depicted in Fig. 3 point out a “burst” stage during the 1st day leading to the release of 56 ± 6 % (3.29 ± 0.35 µmol) of the payload. This step was followed by a sustained release of 391 nmol per day starting from day 1 until the release of

the entire payload after 7 days. Hence, HMPm seem to be adapted to the delivery of APIs that require low plasma concentrations for their systemic activity, such as steroid hormones and their analogs. However, a more sustained release would be interesting in order to reduce the SC injection frequency. One could argue that it can be achieved by increasing the density of the hybrid network since it have been shown that API release from HMP occurs by a diffusion mechanism (Doufène et al., 2019). To set the context in the literature, two examples of estradiol-loaded microparticles subcutaneously injected could be discussed: Guo et *al.* (Guo et al., 2016) synthesized an estradiol-polyketal conjugate and formulated it into microparticles that showed an interesting sustained release of estradiol over 20 weeks. However, the synthesis and purification involved several steps and various organic solvents were used (ether, toluene, tetrahydrofuran, chloroform, hexane, acetonitrile and methanol), and the particles released simultaneously equivalent amounts of acetone and 1,4-cyclohexanedimethanol from the conjugate. In another case, the researchers entrapped estradiol in poly(lactic-co-glycolic acid) (PLGA) microparticles and the *in vitro* release in mini dialysis device took place over 4 weeks. Here again, the same manufacturing disadvantages were reported. Moreover, the degradation of PLGA *in vivo* is well-known to acidify the surrounding cellular environment and may eventually alter the tissues.

Furthermore, it is well-known that the use of different *in vitro* release set-ups can significantly affect the release kinetic profiles (Qureshi and Shabnam, 2001). Regarding the PBS/octanol biphasic system used here, it appeared to be the most biorelevant set-up for such poorly water-soluble API release and, to the best of our knowledge, no study on steroid release in a biphasic system has already been described in the literature (Pestieau et al. 2017).

3.4. *In vitro* activity of estradiol released from the hybrid microparticles

(Fig. 4)

(Table 2)

The suitability of the formulation process was determined by assessing the *in vitro* activity of estradiol released from 12 months old and freshly synthesized HMPm (Fig. 4). The two formulations reached 100 % of the theoretical estradiol activity meaning that the intrinsic activity of the released estradiol was fully preserved in both cases. Moreover, the EC_{50} deduced from the dose-response curves (Table 2) were close to the reference attesting that the affinity of the released estradiol to ERα was also fully maintained. Hence, the chemical structure of the API was not affected by the formulation process, and the entrapped API was stable over 12 months at room temperature highlighting a protective effect of HMPm.

3.5. Cytocompatibility evaluation of the hybrid microparticles

As a prerequisite for the *in vivo* study, the HMPm cytocompatibility was evaluated on NIH 3T3 cell line (Fig. 5). Almost all the cells survived (> 98 %) up to a concentration of 10 $mg \cdot ml^{-1}$ after 24 h exposure to HMPm extracts. The viability decreased to 84 ± 5 % with the upper concentration of HMPm after 48 h exposure, but still being acceptable. This could be explained by the presence of residual carrageenan on HMPm arising from the aqueous phase after washing.

(Fig. 5)

3.6. Biocompatibility evaluation of the hybrid microparticles

For each animal, the one section out of four stained with HES that showed the most severe changes was scored. After 4 days, the aqueous vehicle content (i.e. carboxymethylcellulose and polysorbate) was evidenced inside moderate numbers of vacuolated macrophages in the subcutaneous tissue. However, there was no evidence of vehicle-induced acute or subacute inflammation. For animal treated with HMPm dispersed in the vehicle, the particles could be seen as round imprints of variable sizes surrounded by macrophages, which were the main cell type present to phagocytose them (Fig. 6). However, there was no inflammation as proved by the absence of neutrophils and lymphocytes.

(Fig. 6)

After 28 days, the vehicle was still visible as small amounts of grey transparent amorphous materials surrounded by large numbers of macrophages as seen after 4 days. Multifocally, there was minimal to mild fibrosis confirmed on the section stained with RS (data not shown). The sites injected with the HMPm were characterized by variable amounts of grey transparent materials and several rounded clear spaces (imprints) surrounded by walls of vacuolated macrophages and occasionally thin strands of collagen (consistent with minimal to mild fibrosis) (Fig. 7).

(Fig. 7)

A global score was given to reflect the overall host tissue reaction based on the most marked parameter (mainly macrophagic reaction and fibrosis, Table 3). At day 4, the severity was deemed moderate for the vehicle alone and marked for the HMPm suspension. After 28 days, there was no real difference between the vehicle and the HMPm suspension (both marked) (Fig. 8).

(Fig. 8)

(Table 3)

Overall, the histopathologic examination showed that the local tissue reactions elicited by the HMPm and the vehicle were very similar in nature and severity. They both were well tolerated causing an expected and appropriate macrophagic reaction (phagocytosis), but no acute or subacute reaction. The level of lymphocytic infiltration was extremely low. It can be noticed that there was no evolution over time, and that the HMPm tend to migrate as there was no structure, such as a fibrotic capsule, to hold the product in place.

When considering the *in vitro* release time of the entire estradiol payload (i.e. 7 days), the persistence of HMPm after that in tissues would be irrelevant with this model API. Indeed, the HMPm were still present in tissues even after 28 days because of their full biocompatibility. Hence, this may suggest that either an improvement of the API retention would turn the HMPm into a very long-acting drug delivery system, or an enhancement of the microparticle degradability have to be studied. The HMPm could potentially degrade under the action of enzymes and generate metabolizable fatty acids, glycerol, and small chains of siloxanes (less than 7% of the entire mass). The latter compounds require longer degradation time lasting several months by oxidation/hydrolysis mechanisms inside macrophages, as described by Pfeiderer et al. (Pfleiderer et al., 1999). Indeed, they are uptaken by macrophages present in all tissues, and under the action of reactive oxygen metabolites generated by macrophages, they are biotransformed in functional groups containing silicon atoms bound to three or four oxygens. Such metabolites are then transported to organs (i.e. liver, kidneys) and excreted. If the microparticle biodegradation does not take place over a suitable period of time, their

elimination is consequently delayed. An alternative would be the development of monolithic and removable drug delivery devices made of ICOm.

4. Conclusion

New hybrid microparticles were synthesized in two steps consisting of a silylation of castor oil then an emulsification throughout a thermostabilized emulsion process. In order to reduce the environmental impact, the green process requirements were fully complied here since no catalyst and no solvents other than water were used, thanks to the high sol-gel reactivity of ICOm. Resulting HMPm were 80 µm sized and presented high condensation yield and degree reflecting the crosslinking quality, and when loaded with estradiol, they showed a satisfying effective loading. Moreover, the HMPm demonstrated a complete stability at room temperature, and the entrapped API was unaltered over 12 months. Release kinetics in a PBS/octanol biphasic system exhibited a one-week release profile, and the released estradiol was fully active on HELN ERα cells pointing out the suitability of the formulation process. Finally, the HMP demonstrated their safety through their cytocompatibility on NIH 3T3 fibroblasts (ISO 10993-5 standard) and their full biocompatibility after subcutaneous injection on mice (ISO 10993-6 standard). Hence, HMPm proved to be a promising green and biocompatible drug delivery system that can substantially contribute in the area of long-acting and subcutaneously delivered systems.

Acknowledgements

Authors thank the Algerian government for the Ph.D. grant to Koceïla Doufène and the Franco-Algerian steering committee for its support. The authors are willing to thank Emmanuel Fernandez (ICGM), Xavier Garric, Audrey Bethry and Magali Gary-Bobo

(IBMM), Yoan Buscail (RHEM) and Catherine Botteron (Sirius Pathology) for their precious support in accomplishing the study.

Liquid-state NMR analyses were performed by the “Laboratoire de Mesures Physiques” - analytical facilities of Montpellier University, the histological sections were prepared and stained in the “Réseau d’Histologie Expérimentale de Montpellier” - RHEM facility supported by SIRIC Montpellier Cancer (Grant INCa_Inserm_DGOS_12553) and the european regional development foundation and the occitanian region (FEDER-FSE 2014-2020 Languedoc Roussillon), and the histology interpretation was carried out in Sirius Pathology.

References

Al Durdunji, A., AlKhatib, H.S., Al-Ghazawi, M., 2016. Development of a biphasic dissolution test for Deferasirox dispersible tablets and its application in establishing an in vitro–in vivo correlation. Eur. J. Pharm. Biopharm. 102, 9–18. https://doi.org/10.1016/j.ejpb.2016.02.006

Bellet, V., Hernandez-Raquet, G., Dagnino, S., Seree, L., Pardon, P., Bancon-Montiny, C., Fenet, H., Creusot, N., Aït-Aïssa, S., Cavailles, V., Budzinski, H., Antignac, J.-P., Balaguer, P., 2012. Occurrence of androgens in sewage treatment plants influents is associated with antagonist activities on other steroid receptors. Water Res. 46, 1912–1922. https://doi.org/10.1016/j.watres.2012.01.013

Bittner, B., Richter, W., Schmidt, J., 2018. Subcutaneous Administration of Biotherapeutics: An Overview of Current Challenges and Opportunities. BioDrugs 32, 425–440. https://doi.org/10.1007/s40259-018-0295-0

Chen, W., Yung, B.C., Qian, Z., Chen, X., 2018. Improving long-term subcutaneous drug delivery by regulating material-bioenvironment interaction. Adv. Drug Deliv. Rev. 127, 20–34. https://doi.org/10.1016/j.addr.2018.01.016

Collins, D.S., Sánchez-Félix, M., Badkar, A.V., Mrsny, R., 2020. Accelerating the development of novel technologies and tools for the subcutaneous delivery of biotherapeutics. J. Controlled Release 321, 475–482. https://doi.org/10.1016/j.jconrel.2020.02.036

Delfosse, V., Grimaldi, M., Pons, J.-L., Boulahtouf, A., le Maire, A., Cavailles, V., Labesse, G., Bourguet, W., Balaguer, P., 2012. Structural and mechanistic insights into bisphenols action provide guidelines for risk assessment and discovery of bisphenol A substitutes. Proc. Natl. Acad. Sci. 109, 14930–14935. https://doi.org/10.1073/pnas.1203574109

Denninger, A., Westedt, U., Rosenberg, J., Wagner, K.G., 2020. A Rational Design of a Biphasic Dissolution Setup—Modelling of Biorelevant Kinetics for a Ritonavir Hot-Melt Extruded Amorphous Solid Dispersion. Pharmaceutics 12, 237. https://doi.org/10.3390/pharmaceutics12030237

Doufène, K., Lapinte, V., Gaveau, P., Félix, G., Cacciaguerra, T., Chopineau, J., Robin, J.-J., Devoisselle, J.-M., Aubert-Pouëssel, A., 2019. Tunable vegetable oil / silica hybrid microparticles for poorly water-soluble drug delivery. Int. J. Pharm. 118478. https://doi.org/10.1016/j.ijpharm.2019.118478

Gao, Z., Crowley, W.R., Shukla, A.J., Johnson, J.R., Reger, J.F., 1995. Controlled Release of Contraceptive Steroids from Biodegradable and Injectable Gel Formulations: In Vivo Evaluation. Pharm. Res. 12, 864–868. https://doi.org/10.1023/A:1016261004230

Guo, S., Nakagawa, Y., Barhoumi, A., Wang, W., Zhan, C., Tong, R., Santamaria, C., Kohane, D.S., 2016. Extended Release of Native Drug Conjugated in Polyketal Microparticles. J. Am. Chem. Soc. 138, 6127–6130. https://doi.org/10.1021/jacs.6b02435

Hernández-Ruiz, V., Forestier, E., Gavazzi, G., Ferry, T., Grégoire, N., Breilh, D., Paccalin, M., Goutelle, S., Roubaud-Baudron, C., 2020. Subcutaneous Antibiotic Therapy: The Why, How, Which Drugs and When. J. Am. Med. Dir. Assoc. S1525861020303637. https://doi.org/10.1016/j.jamda.2020.04.035

Jones, G.B., Collins, D.S., Harrison, M.W., Thyagarajapuram, N.R., Wright, J.M., 2017. Subcutaneous drug delivery: An evolving enterprise. Sci. Transl. Med. 9, eaaf9166. https://doi.org/10.1126/scitranslmed.aaf9166

Kalicharan, R.W., Oussoren, C., Schot, P., de Rijk, E., Vromans, H., 2017. The contribution of the in-vivo fate of an oil depot to drug absorption. Int. J. Pharm. 528, 595–601. https://doi.org/10.1016/j.ijpharm.2017.06.055

Loy, D.A., Baugher, B.M., Baugher, C.R., Schneider, D.A., Rahimian, K., 2000. Substituent Effects on the Sol−Gel Chemistry of Organotrialkoxysilanes. Chem. Mater. 12, 3624–3632. https://doi.org/10.1021/cm000451i

Pestieau, A. Evrard, B., 2017. In vitro biphasic dissolution tests and their suitability for establishing in vitro-in vivo correlations: A historical review. Eur. J. Pharm. Sci. 102, 203-219. https://doi.org/10.1016/j.ejps.2017.03.019

Pfleiderer, B., Moore, A., Tokareva, E., Ackerman, J.L., Garrido, L., 1999. Biodegradation of polysiloxanes in lymph nodes of rats measured with 29Si NMR. Biomaterials 20, 561–571. https://doi.org/10.1016/S0142-9612(98)00208-7

Phillips, D.J., Pygall, S.R., Cooper, V.B., Mann, J.C., 2012a. Overcoming sink limitations in dissolution testing: a review of traditional methods and the potential utility of biphasic systems. J. Pharm. Pharmacol. 64, 1549–1559. https://doi.org/10.1111/j.2042-7158.2012.01523.x

Phillips, D.J., Pygall, S.R., Cooper, V.B., Mann, J.C., 2012b. Toward Biorelevant Dissolution: Application of a Biphasic Dissolution Model as a Discriminating Tool for HPMC Matrices Containing a Model BCS Class II Drug. Dissolution Technol. 19, 25–34. https://doi.org/10.14227/DT190112P25

P.V., J., Nair, S.V., Kamalasanan, K., 2017. Current trend in drug delivery considerations for subcutaneous insulin depots to treat diabetes. Colloids Surf. B Biointerfaces 153, 123–131. https://doi.org/10.1016/j.colsurfb.2017.02.017

Qureshi, S.A., Shabnam, J., 2001. Cause of high variability in drug dissolution testing and its impact on setting tolerances. Eur. J. Pharm. Sci. 12, 271–276. https://doi.org/10.1016/S0928-0987(00)00174-3

Riffkin, C., Huber, R., Keysser, C.H., 1964. Castor Oil as a Vehicle for Parenteral Administration of Steroid Hormones. J. Pharm. Sci. 53, 891–895. https://doi.org/10.1002/jps.2600530809

Sav, A., King, M.A., Whitty, J.A., Kendall, E., McMillan, S.S., Kelly, F., Hunter, B., Wheeler, A.J., 2015. Burden of treatment for chronic illness: a concept analysis and review of the literature. Health Expect. 18, 312–324. https://doi.org/10.1111/hex.12046

544 Strickley, R.G., 2004. Solubilizing Excipients in Oral and Injectable Formulations. Pharm.
545 Res. 21, 201–230. https://doi.org/10.1023/B:PHAM.0000016235.32639.23

546 Vintiloiu, A., Leroux, J.-C., 2008. Organogels and their use in drug delivery — A review. J.
547 Controlled Release 125, 179–192. https://doi.org/10.1016/j.jconrel.2007.09.014

548 Viola, M., Sequeira, J., Seiça, R., Veiga, F., Serra, J., Santos, A.C., Ribeiro, A.J., 2018.
549 Subcutaneous delivery of monoclonal antibodies: How do we get there? J. Controlled
550 Release 286, 301–314. https://doi.org/10.1016/j.jconrel.2018.08.001

551

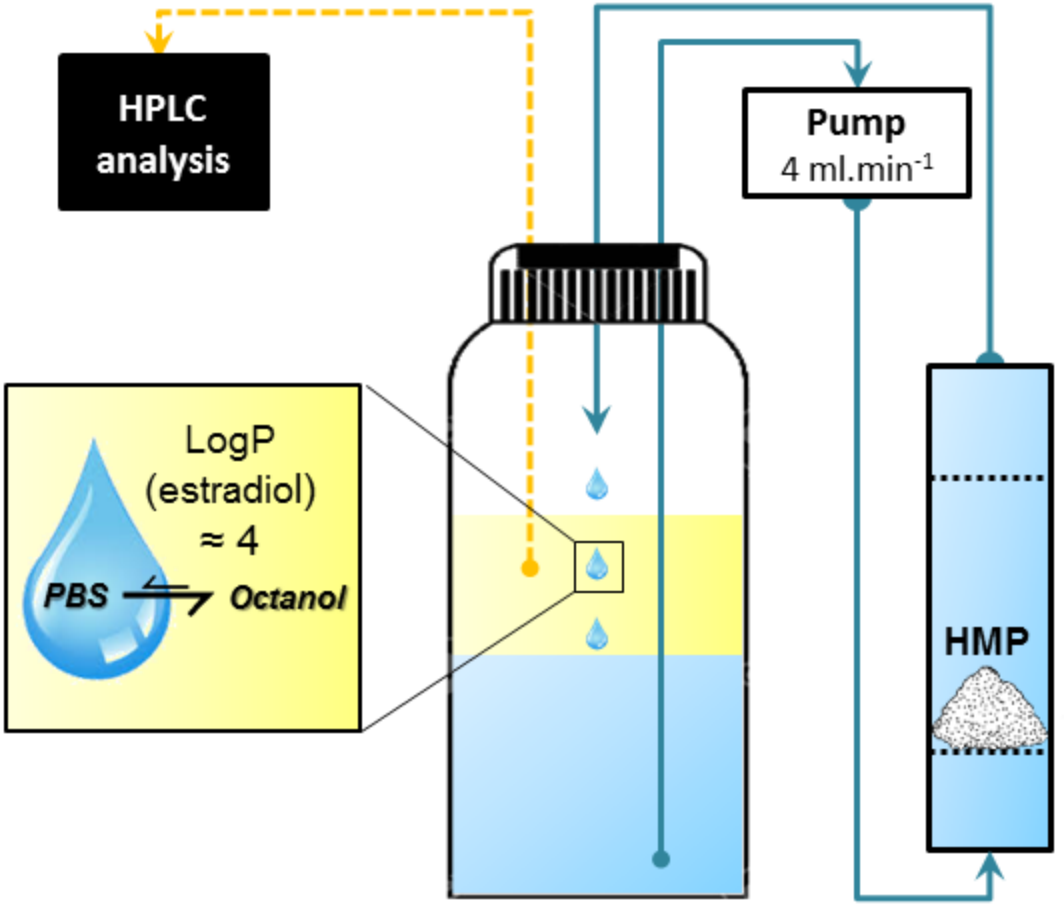
HPLC analysis
Pump
4 ml.min-1
LogP (estradiol) ≈ 4
PBS
Octanol
HMP

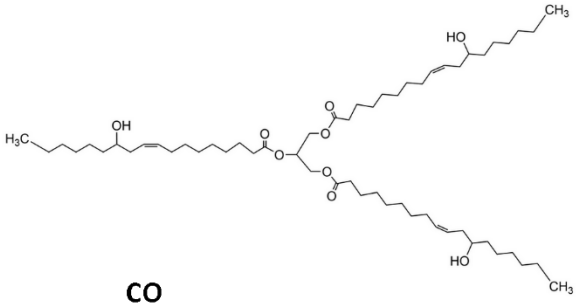

CO

60 °C , 72h

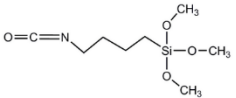

IPTMS

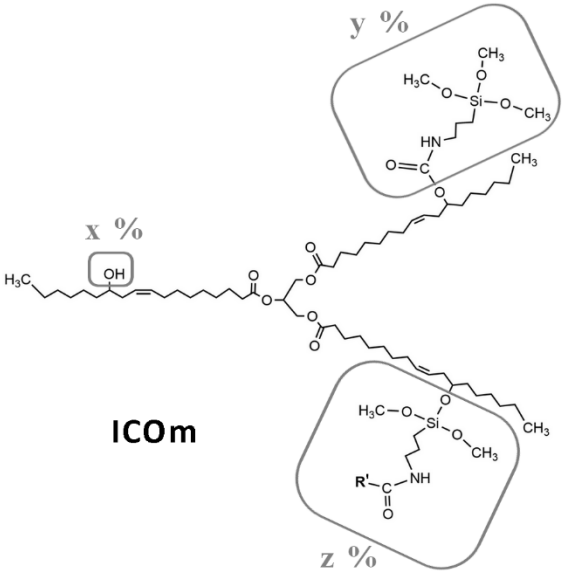

ICOm

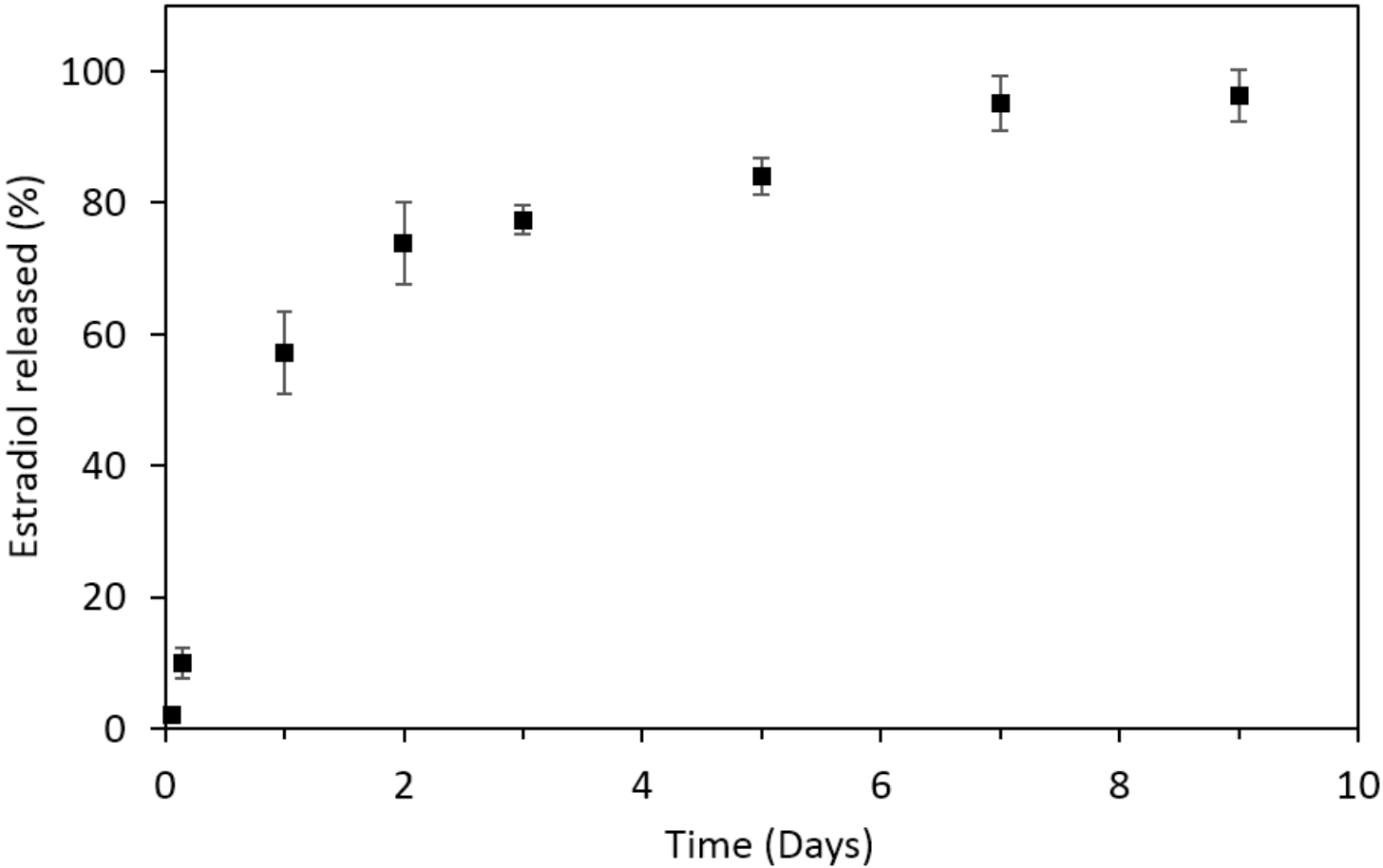
Estradiol released (%)
100
80
60
40
20
0
0
2
4
6
8
10
Time (Days)

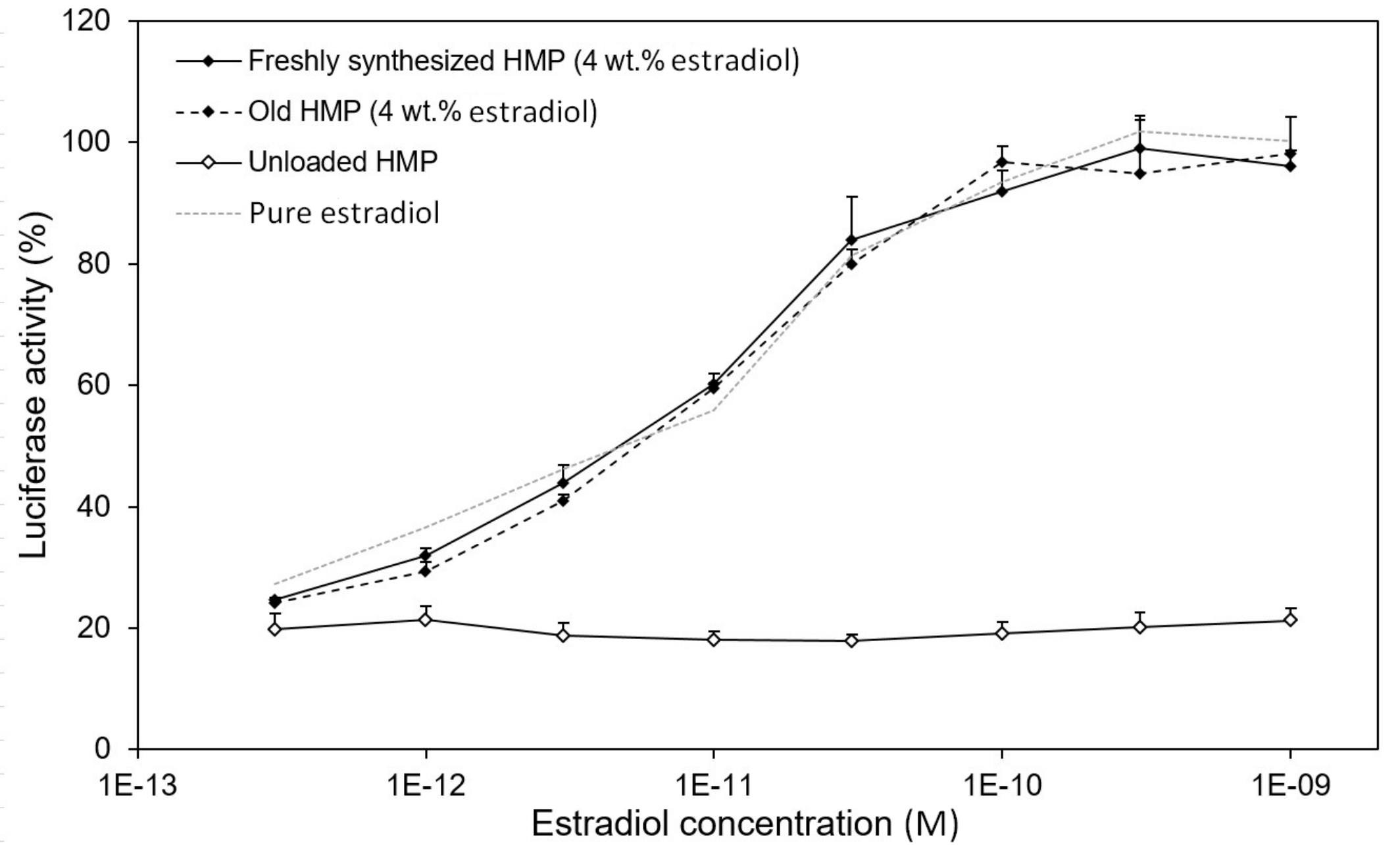
Freshly synthesized HMP (4 wt.% estradiol)
Old HMP (4 wt.% estradiol)
Unloaded HMP
Pure estradiol
Luciferase activity (%)
120
100
80
60
40
20
0
1E-13
1E-12
1E-11
1E-10
1E-09
Estradiol concentration (M)

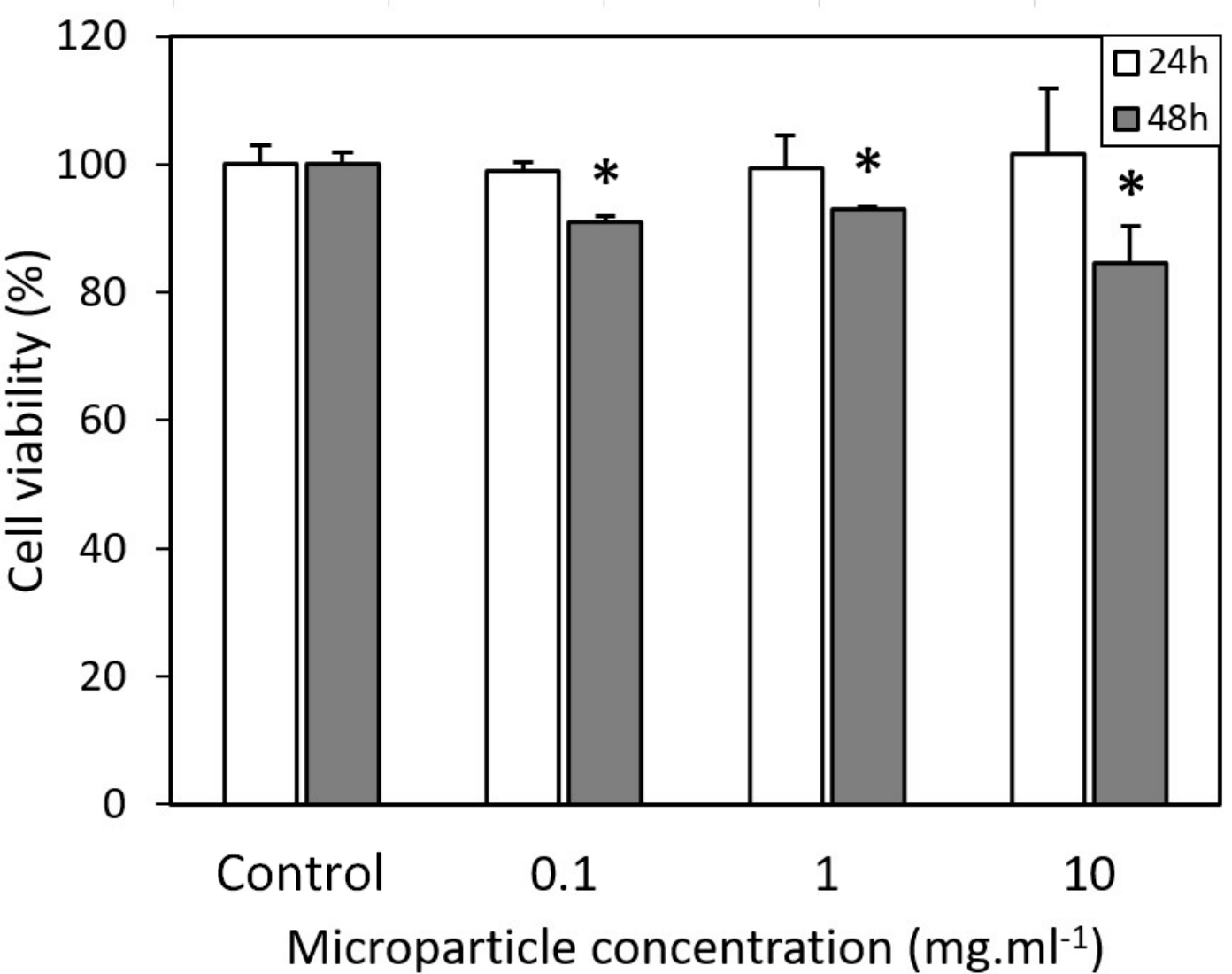
120
100
80
60
40
20
0
Cell viability (%)
24h
48h
*
*
*
Control
0.1
1
10
Microparticle concentration (mg.ml-1)

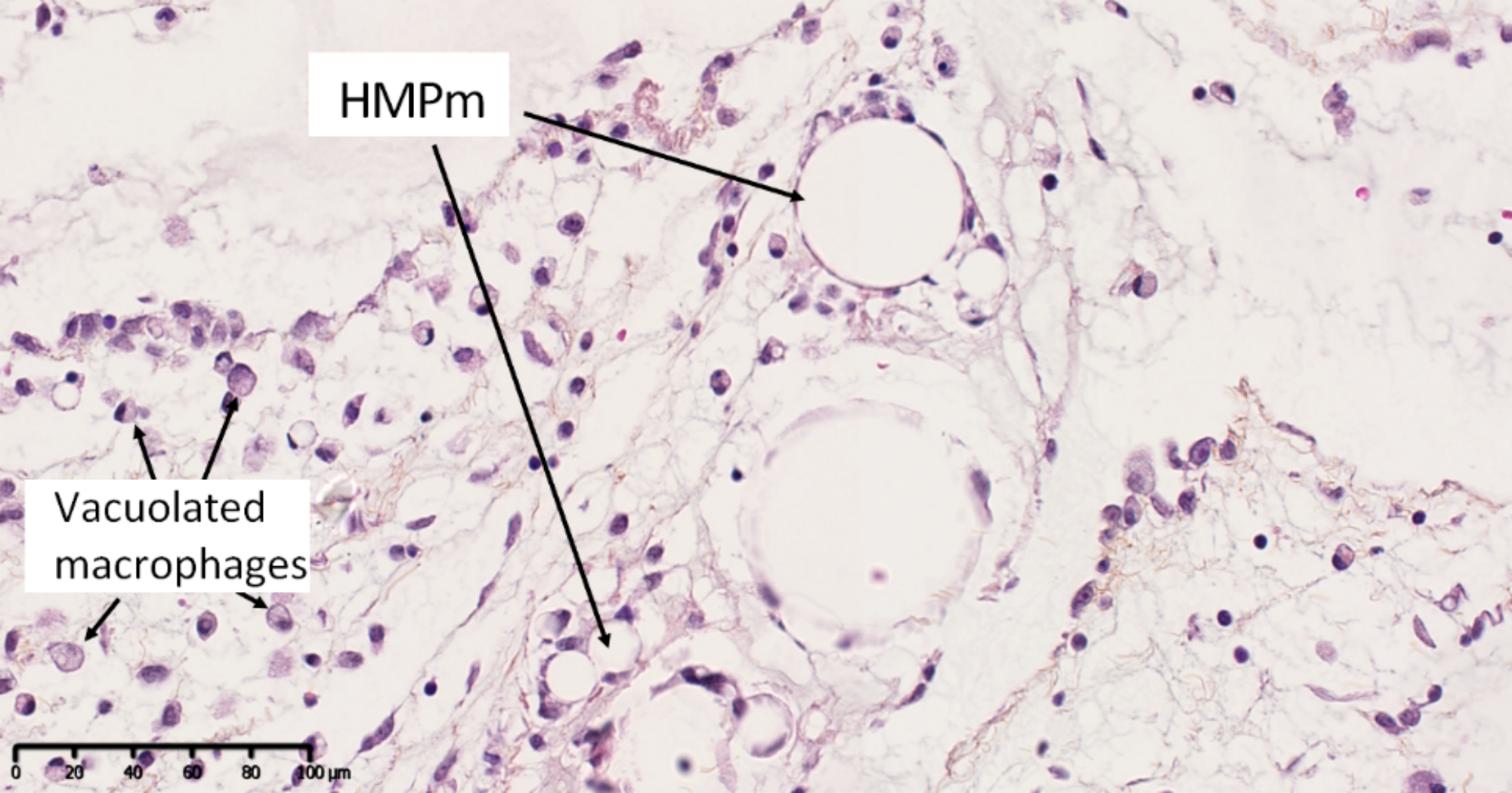
HMPm
Vacuolated macrophages
0
20
40
60
80
100 µm

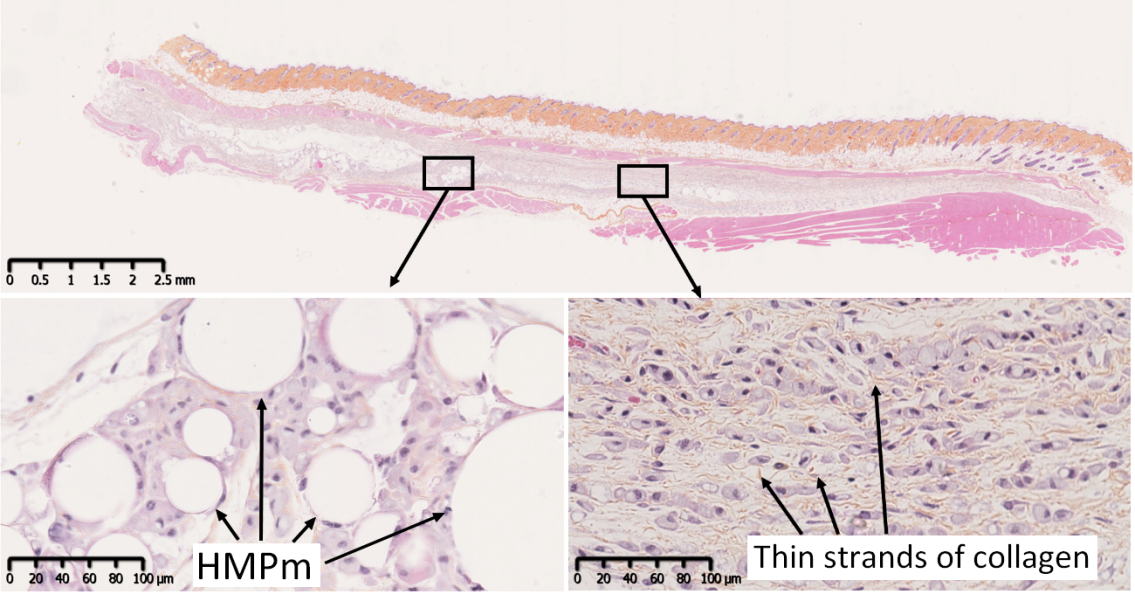
0 0.5 1 1.5 2 2.5 mm
0 20 40 60 80 100 µm
HMPm
0 20 40 60 80 100 µm
Thin strands of collagen

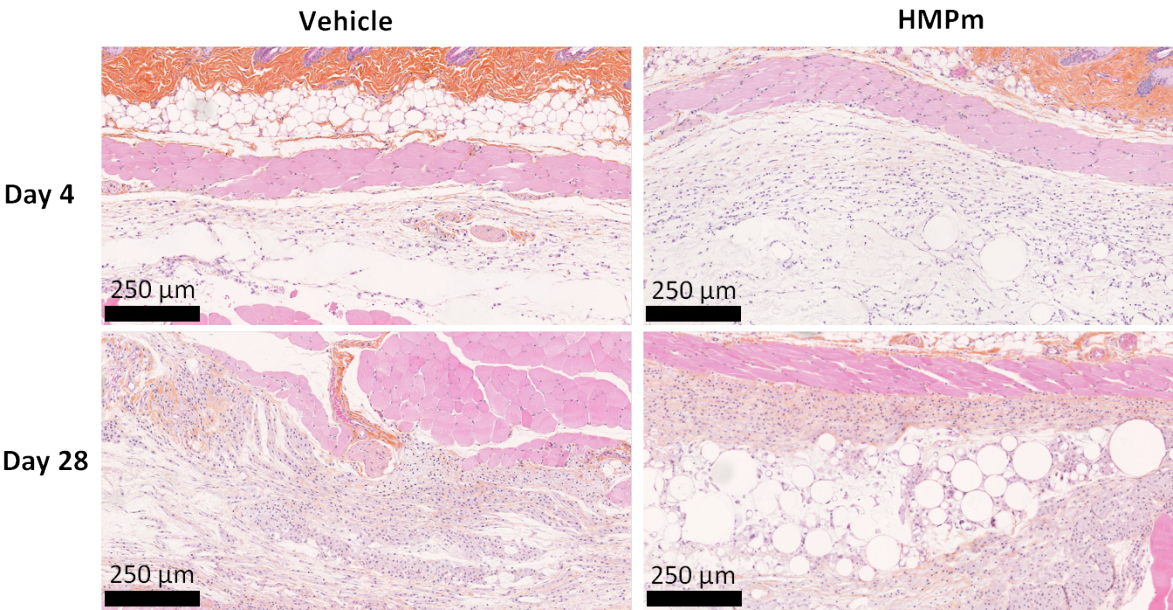
Vehicle
HMPm
Day 4
Day 28
250 µm
250 µm
250 µm
250 µm

Table 1. Solid-state ^{29}Si NMR results of the HMPm sample analysis. CY and CD were calculated as follows: $\mathrm{CY} = 100\,\% - \mathrm{LP}\,;\ \mathrm{CD} = \frac{T^1+2\cdot T^2+3\cdot T^3}{3\cdot \mathrm{CY}}$. CD: condensation degree, CY: condensation yield, LP: liquid peak.

^{29}Si signal (%)					**CY (%)**	**CD (%)**
Liquid peak *-45 ppm*	T^0 *-49 ppm*	T^1 *-54 ppm*	T^2 *-58 ppm*	T^3 *-67 ppm*		
14.98	4.22	4.33	32.51	43.89	85	79

Table 2. EC_{50} of pure estradiol and estradiol released from HMPm on HELN Erα cells.

Sample	**EC_{50} ($\times 10^{-12}$ M)**
Pure estradiol	7.3 ± 0.07
Freshly synthesized HMPm (4 wt.% estradiol)	6.2 ± 0.03
Old HMPm (4 wt.% estradiol)	6.2 ± 0.03

Table 3. Summary of the histopathology scores (mean of n = 3 for vehicles and n = 6 for HMPm, NA: not applicable).

Time period	**Group**	**Neutrophils**	**Lymphocytes**	**Plasma cells**	**Macrophages**	**Giant cells**	**Necrosis**	**Fibrosis**	**Fibrin**	**Cell or tissue degeneration**	**Tissue integration**	**Tissue ingrowth**	**Global score**
Day 4	**Vehicle**	0	0.3	0	2	0	0	0	0	0.3	NA	NA	**2**
	HMPm	0.1	1	0	3	0.4	0	0	0	0.3	NA	NA	**3**
Day 28	**Vehicle**	0	0.3	0	3	0	0	1	0	0	1	1	**3**
	HMPm	0	0.5	0	2.7	0.3	0	1	0	0	1	1	**2.7**

Silica

Green Chemistry & Process

Castor oil

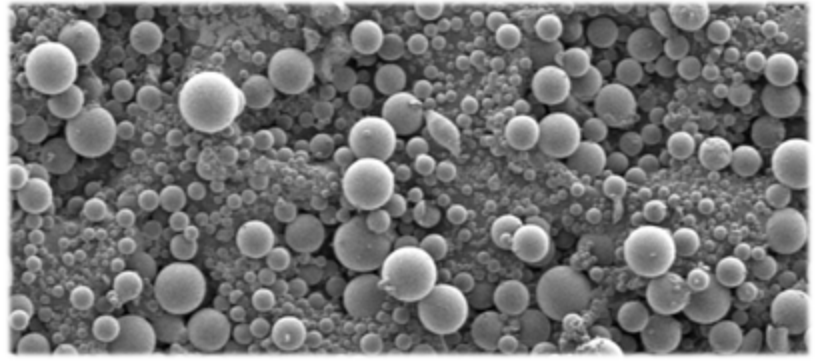

Hybrid microparticles

Estradiol loading

Sustained Drug Delivery

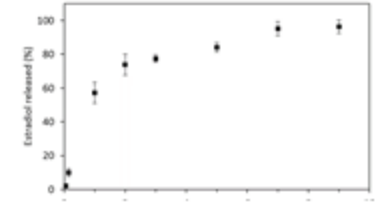

Drug Activity

Estradiol

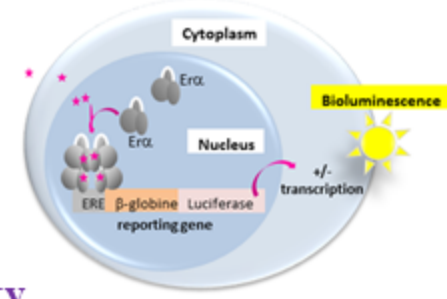

Biocompatibility

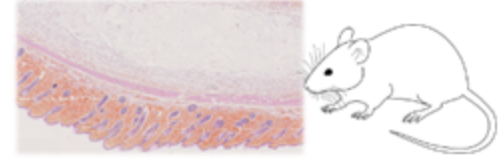

Drug Delivery System for Subcutaneous Administration